



VEHICLE DESIGN PORTFOLIO

EXPERIMENTAL VALIDATION
AND DESIGN OPTIMISATION
OF AERODYNAMICS AND
HEAT TRANSFER SYSTEMS

LARA MERICAN

PROJECT SUMMARY

INTRODUCTION

This section of the portfolio presents the **aerodynamic analysis** of a vehicle using **wind tunnel testing** in order to verify the results of the Computational Fluid Dynamics (CFD) analysis.

KEY OUTCOMES

6.56
**DISPARITY IN DRAG
COEFFICIENT (%)**

The drag coefficient value obtained from CFD analysis testing **closely matched** the value calculated from the wind tunnel experiment.

METHODOLOGY

One vehicle design from our group was chosen to be **3D printed**. A **wind tunnel test** was carried out and results were compared to **CFD analysis results**. Following on from this, **design optimisation** suggestions were made.

130
**DISPARITY IN LIFT
COEFFICIENT (%)**

The lift coefficient value evaluated from the wind tunnel test exhibited a **critical disparity**. This could possibly be due to differences in **Reynolds number** and **weight**.

KEY DESIGN FEATURES



- **Smooth Contour:** The smooth profile reduces flow separation, thus reducing air resistance and encouraging laminar flow.
- **Back Wheel Cover:** The back wheel is fully concealed, encouraging laminar flow.
- **Elongated Tail:** Tapering and elongating the tail reduces wake turbulence at the rear end.
- **Spats:** Located in front of the front wheel to direct airflow around wheels, thus minimising turbulence.
- **Flat Underbody:** Creates a low pressure region which increases down force and prevents turbulence.
- **Rear Diffuser:** Creates a low pressure region below the car with a high pressure region above to increase downforce.
- **Three Wheel Design:** Allows for sharp rear taper, reducing flow separation.
- **Smooth Mirror Finish:** Minimises surface roughness.

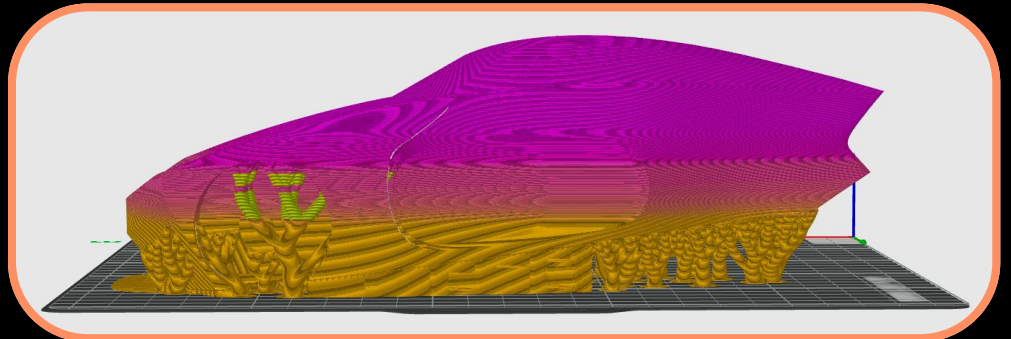
3D PRINTING OF CONCEPT MODEL

The setup was designed to **maximise print quality**, replicating the **smooth surface** of the simulated car. This ensures the wind tunnel test closely matches the simulation results.



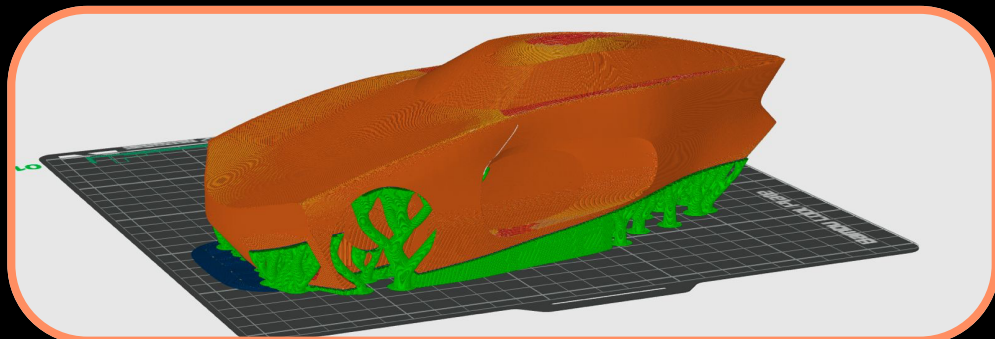
5° INCLINE

The car was inclined by 5°, increasing the number of **layer lines** on the front hood and windscreen, resulting in a **smoother surface finish**.



VARIABLE LAYER LINE HEIGHT

The layer height varies from 0.2 mm at the bottom to 0.1 mm at the top, **optimising print speed** while ensuring **high quality in critical areas**.



TREE SUPPORTS

Tree supports were used for **overhangs** as they are easy to remove and their branching structure provides the necessary **support** while minimising contact with the print.



PRINTED WITH X1 CARBON

Produces **high quality** parts at very **high speed**. It could have been improved further by **wet sanding and polishing** the model to **reduce surface abnormalities** and **skin friction**.

WIND TUNNEL TESTING

When setting up the wind tunnel test, several parameters must be set to ensure that the test results are accurate, representative of the real world, and complementary to the CFD results previously calculated.

CAR SIZE

The car must be scaled down appropriately for two reasons:

1. It must be small enough to print
2. It must be small enough to avoid blockage effects - where the flow around the car is artificially accelerated due to limited space between the car and the walls

Generally, a blockage ratio of **less than 5-10%** is acceptable (He et al., 2022). The dimensions of the wind tunnel used are **0.914 × 0.914 × 5m** (Imperial College London, n.d.). By scaling down the car to 1/18 scale, it is small enough to print and has a blockage ratio of only 0.69%.

APPROPRIATE WIND TUNNEL SENSORS

The wind tunnel used for the experimenting is the **T1 wind tunnel** which is equipped with "**vibration isolation**" and a **high-precision 3-axis traverse**" (Imperial College London, n.d.). This makes them perfect for measuring the **drag**, **lift** and **side forces** on the car to compare them with the **CFD results**.

WIND VELOCITY

The wind velocity in the tunnel was **carefully calibrated** to match the CFD simulation conditions as closely as possible. Ensuring consistency in wind velocity is crucial for obtaining **reliable aerodynamic data**, especially when comparing drag and lift values with CFD results.

CAR YAW & LEVELLING

It is important that the platform the car is mounted on is as level as possible to accurately replicate the **pitch** and **yaw** from the **CFD simulation**. The test section of the **T1 wind tunnel** is **self-levering**, helping to ensure zero pitch and yaw. While testing different **yaw angles** (conducting a **yaw sweep**) would provide insights into how **drag** and **lift** coefficients vary under real driving conditions, this was beyond the scope of the module.

RIDE HEIGHT

Airflow under the car can significantly effect the turbulent wake, the underbody pressure and the ground effect. To ensure this, the car has been bolted directly to an aluminium on the floor of the wind tunnel.

AMBIENT ENVIRONMENTAL VARIABLES

The parameters of the wind tunnel were set to closely replicate the setup for the simulation.

Environment Setup In Simulation

Wind Velocity	30.5 m/s
Ambient pressure	101,325 Pa
Ambient temperature	288.16 K

Environment Setup In Wind Tunnel

Wind Velocity	30.606 m/s
Ambient pressure	101,620 Pa
Ambient temperature	294.27 K

STEP BY STEP PROCEDURE

① HEAT SET INSERTS



Heat-set inserts were added to the 3D printed vehicle to ensure secure connections to the aluminium plate. This ensures bolts can be **securely attached** to the car.

② MOUNT VEHICLE TO PLATE



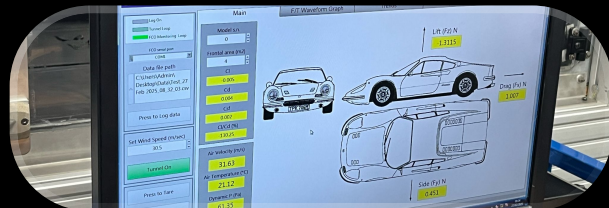
The vehicle is **securely mounted** to an aluminium plate using **bolts**. This prevents the car from detaching during testing and potentially damaging the wind tunnel.

③ MOUNT PLATE IN TUNNEL



The aluminium plate can be mounted to the **load cells** inside the wind tunnel which are used to measure the various **forces**.

④ ENVIRONMENT VARIABLES



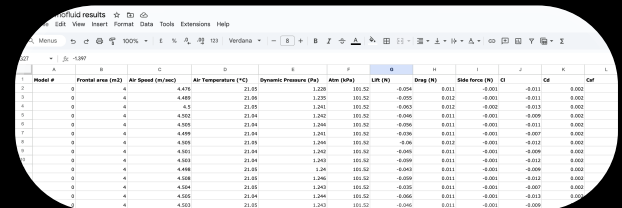
The **ambient temperature** and pressure are set to correspond with the simulation. The wind speed is set to 18 m/s and 30 m/s to measure the drag and lift coefficients for multiple wind speeds.

⑤ 60s WIND TUNNEL RUN



Close off the wind tunnel and run the simulation. This ensures **no external or environmental factors** can influence the results.

⑥ MEASURE DRAG AND LIFT



Sensors around the wind tunnel are used to measure the forces exerted on the car in the **x**, **y** and **z** directions. This corresponds to the **drag**, **lift** and **side**.

Unfortunately, the decision to add a **tuft test** was made after our groups wind tunnel test. As a result, we have no way of comparing airflow over the car in the wind tunnel to the simulated CFD results.

RESULTS COMPARISON

FRONTAL AREA

The full-scale model has a frontal area of 1.876 m^2 . Hence 1/18th scale model has a frontal area of:

$$A = \frac{1.876}{18^2} = 0.0579 \text{ m}^2$$

DRAG COEFFICIENT

Using the measured drag force from the wind tunnel results, we can calculate the drag coefficient:

$$C_d = \frac{2F_d}{\rho v^2 A}$$

$F_d = \text{drag force (N)}$
 $\rho = \text{air density (kg/m}^3)$
 $v = \text{air velocity (m/s)}$
 $A = \text{frontal area (m}^2)$

$$C_d = \frac{2 \times 0.809}{1.225 \times 30.606^2 \times 0.00579}$$

$$C_d = 0.244$$

LIFT COEFFICIENT

Using the measured lift force from the wind tunnel results, we can calculate the lift coefficient:

$$C_l = \frac{2L}{\rho v^2 A}$$

$L = \text{lift force (N)}$
 $\rho = \text{air density (kg/m}^3)$
 $v = \text{air velocity (m/s)}$
 $A = \text{frontal area (m}^2)$

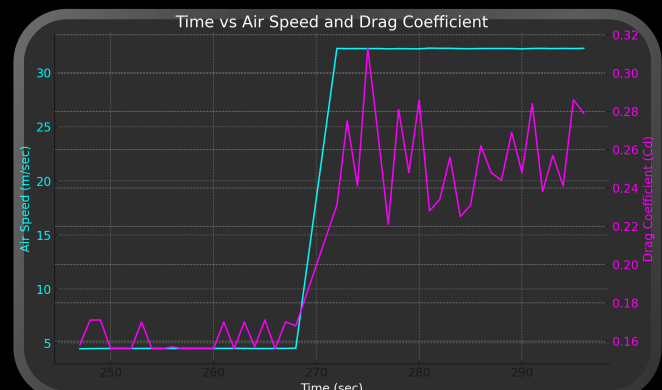
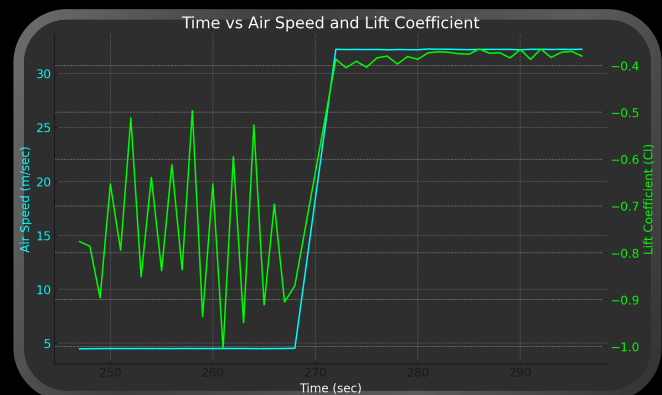
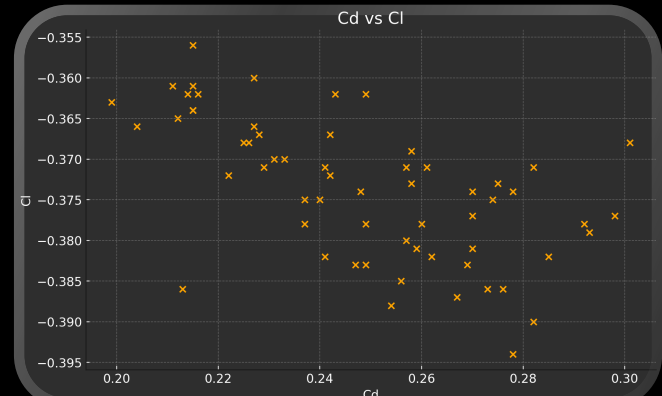
$$C_l = \frac{2 \times (-1.216)}{1.225 \times 30.606^2 \times 0.00579}$$

$$C_l = -0.366$$

WIND TUNNEL VS CFD RESULTS

Design Variation	CFD Simulation	Wind Tunnel	Disparity (%)
Drag Coefficient	0.260	0.244	6.56
Lift Coefficient	0.120	-0.366	130

Note: Disparity is calculated with the wind tunnel result as the reference.



RESULTS ANALYSIS

LIMITATIONS OF OUR WIND TUNNEL

Due to technical problems with the wind tunnel, we were **unable to use a smoke stream** to help analyse streamlines and airflow around the vehicle. Likewise, we were **unable to use traditional, manual methods**, such as the addition of thread or tape to the vehicle, to aid airflow visualisation.

This limits the depth of analysis that we can conduct. Our only **experimentally obtained results are lift and drag forces**, and so these are the only factors that we can compare to CFD simulation results.

DRAG COEFFICIENT DISPARITY (6.56%)

In general, the drag coefficient showed reasonable agreement, with the theoretical CFD result being less than 10% away from the experimental wind tunnel result. However, there is still a slight discrepancy which could have been caused by the following:

- **k- ϵ Turbulence Model Limitations:** The model may have over-predicted turbulence intensity, leading to **larger wake regions and higher drag**.
- **Model Quality:** The underside of the 3D printed model exhibited poor quality with **surface roughness and layer sagging**, in contrast to the CFD simulation's perfectly smooth surfaces. This could lead to **different boundary layer behaviours**. However, drag is generally less sensitive to small geometric changes compared to lift, hence explaining the relatively **minor** discrepancy.

LIFT COEFFICIENT DISPARITY (130%)

Not only did the lift coefficient result show a significant magnitude discrepancy, it also showed a change in sign – positive in the CFD result and negative in the wind tunnel result. Though it is difficult to determine the exact cause for discrepancy without airflow visualisation, we can theorise the following reasons:

- **Difference in Reynolds Number:** The length of the full-scale car used in the CFD simulation was **4.1m**, whereas the 1/18th car model had a length of **0.23m**. The corresponding lengths can be used to calculate the Reynolds number for both the CFD simulation and wind tunnel experiment. This results in: $Re_{CFD} = 8.46 \times 10^6$ and $Re_{WT} = 4.76 \times 10^5$, which shows the wind tunnel Reynolds number being around **18 times smaller** than the one used in the CFD simulation. The lower Reynolds number in the wind tunnel results in **more laminar boundary layers, earlier flow separation and different vortex formation**.
- **Model Quality:** As described before, the **roughness and layer sagging** on the underside of the 3D printed car may have had an effect on the coefficients. Particularly for the lift coefficient, this may have potentially **increased the downforce** in the wind tunnel, explaining why the lift coefficient is **negative**.
- **Model Weight:** The weight of the car and bolts were **not accounted for** in the wind tunnel test, which would lead to an **overestimation** of lift. However, the result of lift coefficient came out negative, so this may not have had a large effect on the result.

DESIGN OPTIMISATION

SUMMARY

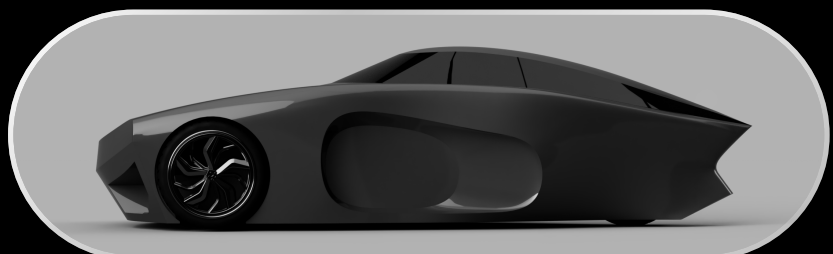
To conclude, the drag and lift coefficients obtained from both the wind tunnel experiment and the CFD simulation indicate that the car design exhibits **good aerodynamic performance**, with a relatively low drag and a reasonable lift. However, lift may have to be improved.

Key points from results comparison include:

- Drag coefficient showed **reasonable agreement** between CFD and wind tunnel results, with a disparity of only **6.56%**.
- Lift coefficient showed a **significant discrepancy** of **130%**, with a sign change.

Reasons for these discrepancies include:

- Differences in Reynolds number
- **Surface roughness** of the 3D-printed wind tunnel model
- Limitations in **airflow visualisation**
- **k- ϵ Turbulent Model** limitations
- Neglected **model weight** in the wind tunnel experiment



POTENTIAL IMPROVEMENTS

VENTING SLITS

- The back wheel may currently be creating unwanted flow detachment.
- Adding small venting slits may help reduce pressure build-up in the back wheel cover, helping the air flow around the back wheel.

IMPROVING DIFFUSER

- According to the results, the car may currently have too much downforce.
- The diffuser angle may have to be reduced if it is causing more flow acceleration than intended.

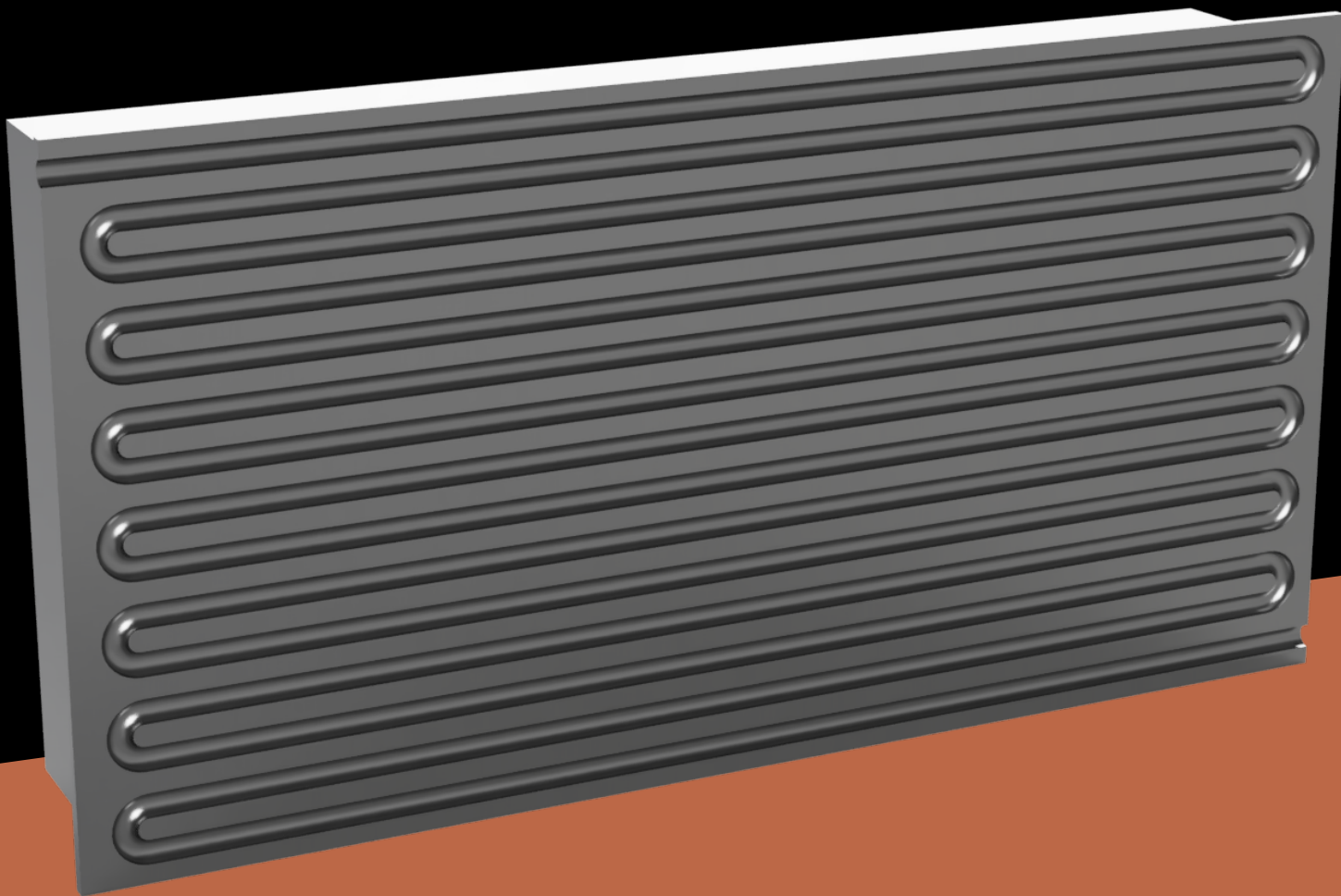
RE-EVALUATING SPATS

- Wheel turbulence can lead to vortex shedding that affects both the drag and lift forces.
- Adjusting the spat shape or positioning could prevent excess vortex generation which will guide airflow better.

PIPELINE DESIGN

EXPERIMENTAL VALIDATION
AND DESIGN OPTIMISATION
OF AERODYNAMICS AND
HEAT TRANSFER SYSTEMS

LARA MERICAN



DESIGN SUMMARY

INTRODUCTION

This section of the portfolio presents the **heat transfer analysis** of a **battery module cooling plate** design for an electric car. It builds upon the pipeline design introduced in the first portfolio, providing a deeper exploration of its **thermal performance and optimisation**.

KEY CFD OUTCOMES

36.1
MAXIMUM TEMPERATURE (°C)

32.8
AVERAGE TEMPERATURE (°C)

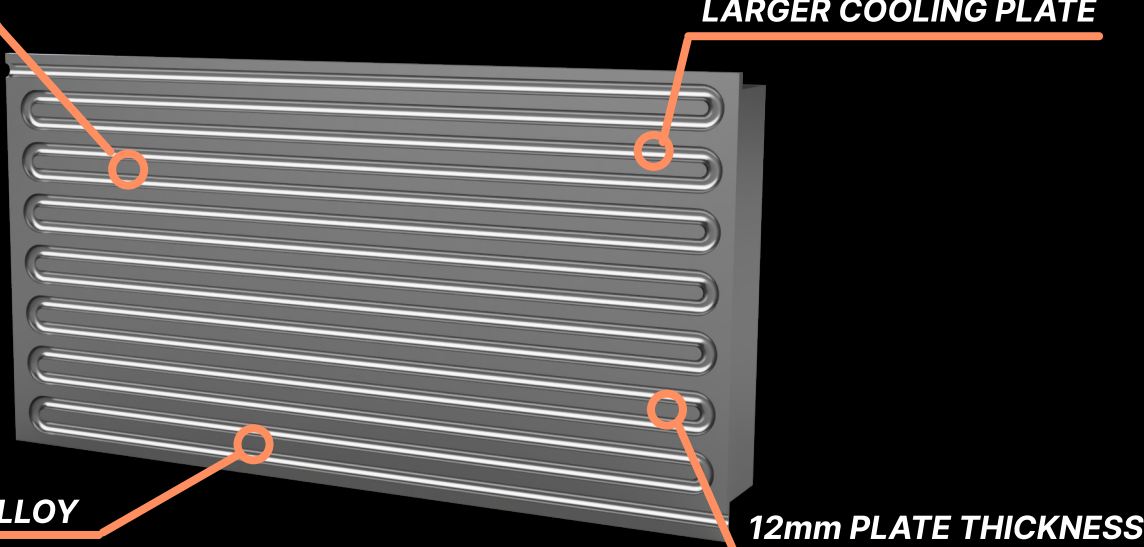
METHODOLOGY

Prior to conducting **Computational Fluid Dynamics (CFD) analysis**, hand calculations were done to estimate the **pressure loss in the pipeline** and the **heat transfer of the cooling plate**. CFD analysis was then carried out at an **initial temperature of 25°C** to analyse the pressure distribution and heat transfer visually and in greater detail.

0.229
MAXIMUM VELOCITY (m/s)

KEY DESIGN FEATURES

SERPENTINE DESIGN



DESIGN VARIATIONS

In order to optimise the design, three variations were tested:

Design Variation 1

- 10mm Cooling Plate Depth
- 7mm Pipe Diameter

Design Variation 2

- 10mm Cooling Plate Depth
- 8mm Pipe Diameter

Design Variation 3

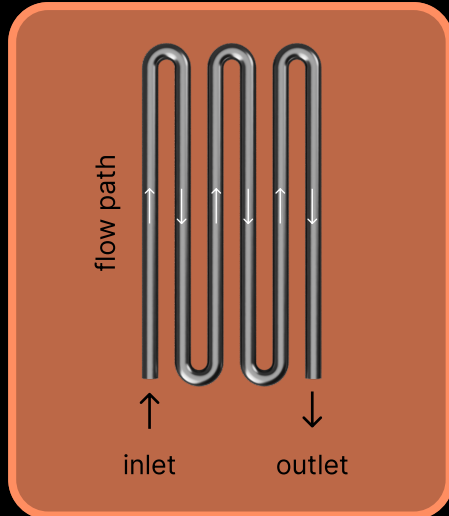
- 12mm Cooling Plate Depth
- 10mm Pipe Diameter

DESIGN RATIONALE

Design Aim: To cool a 420×210×70mm battery module to below 40°C, by designing a cooling plate with one inlet and one outlet. The pipeline design aims to focus on **minimising pressure loss & transferring heat efficiently**.

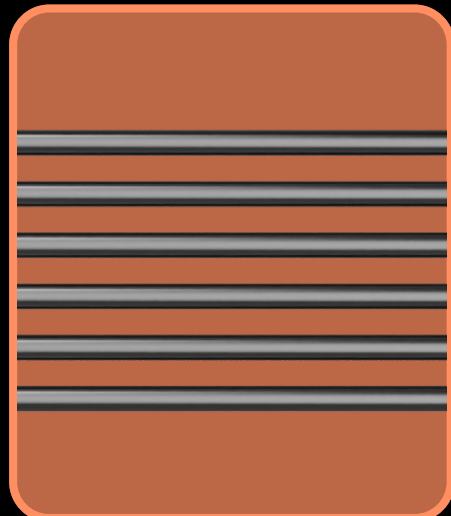
SERPENTINE DESIGN

- Maximises area surface **contact** for heat transfer
- Parallel pipes allow for **uniform cooling distribution**, lower flow resistance and **prevention of flow stagnation**
- Rounded U-bends were used instead of sharp corners to reduce sudden changes in velocity and to **minimise pressure loss**



ALUMINIUM ALLOY

- Lightweight and **corrosion resistant**
- High thermal conductivity of **30 W/m·K** which effectively transfers heat
- Ensures rapid heat spreading which **reduces temperature gradients**



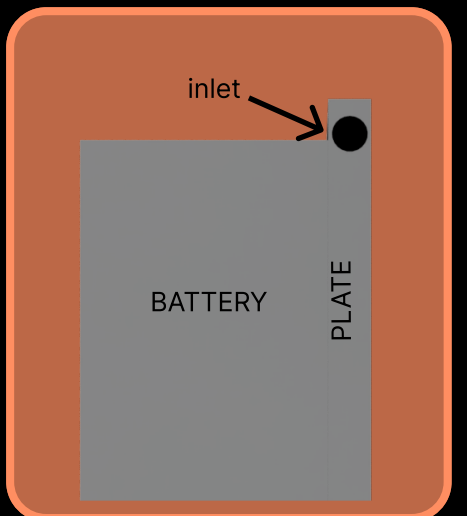
LARGER COOLING PLATE AREA

- The cooling plate size of **440×230×10mm** provides better coverage by maximising the contact area between the plate and the battery
- Allows for more effective **temperature control** and **dissipation** across the battery



12mm PLATE THICKNESS

- A **trade-off** between heat transfer performance and manufacturability
- Optimised for structural integrity to withstand **thermal expansion stresses** and **vibrations** during operation



PRESSURE LOSS IN PIPELINE

Unlikely to be numerically accurate due to many assumptions made, however provides a valuable insight into the trends of pressure loss when varying the design.

GENERAL METHOD

Using the **total pressure loss equation**, we can calculate the pressure loss in the pipeline: $\Delta P_{total} = \Delta P_{major} + \Delta P_{minor}$

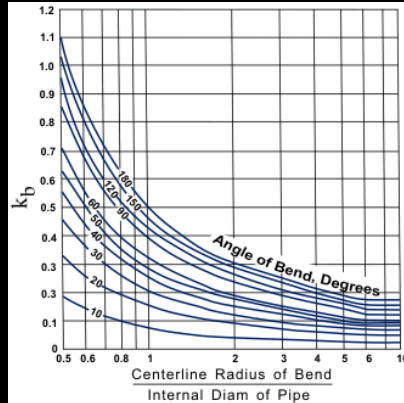
Minor pressure losses (ΔP_{minor}) are due to the U-bends in the design. This is calculated by:

1 LOSS COEFFICIENT VALUE

Identify the loss coefficient value K , by looking on the 180° line at a R/d value of $0.75/d$.

2 EQUATION

$$\Delta P_{minor} = K \cdot \frac{\rho v^2}{2}$$



VARIATION 1 (d=0.007)

$$v = \frac{0.01}{1000 \times \frac{\pi(0.007)^2}{4}} = 0.2598 \text{ m/s}$$

$$Re = \frac{1000 \times 0.2598 \times 0.007}{1.002 \times 10^{-3}} = 1815.28$$

$$f = \frac{64}{1815.28} = 0.0353$$

$$\Delta P_{major} = 0.0353 \cdot \frac{6.37984}{0.007} \cdot \frac{1000 \times 0.2598^2}{2} = 1084.79 \text{ Pa}$$

$$\frac{R}{d} = \frac{0.0075}{0.007} = 1.07 \quad \text{Using the graph, the corresponding loss coefficient value would be } \sim 0.5.$$

$$\Delta P_{minor} = 0.5 \cdot 14 \cdot \frac{1000 \times 0.2598^2}{2} = 236.32 \text{ Pa}$$

$$\Delta P_{total} = 1084.79 + 236.32 = 1321.11 \text{ Pa}$$

VARIATION 2 (d=0.008)

$$v = \frac{0.01}{1000 \times \frac{\pi(0.008)^2}{4}} = 0.1989 \text{ m/s}$$

$$Re = \frac{1000 \times 0.1989 \times 0.008}{1.002 \times 10^{-3}} = 1588.37$$

$$f = \frac{64}{1588.37} = 0.0403$$

$$\Delta P_{major} = 0.0504 \cdot \frac{6.37984}{0.008} \cdot \frac{1000 \times 0.1989^2}{2} = 635.88 \text{ Pa}$$

$$\frac{R}{d} = \frac{0.0075}{0.008} = 0.9375 \quad \text{Using the graph, the corresponding loss coefficient value would be } \sim 0.6.$$

$$\Delta P_{minor} = 0.6 \cdot 14 \cdot \frac{1000 \times 0.1989^2}{2} = 166.23 \text{ Pa}$$

$$\Delta P_{total} = 635.88 + 166.23 = 802.11 \text{ Pa}$$

Major pressure losses (ΔP_{major}) are due to friction along the entire length of the pipe, calculated in order by:

1 FLOW VELOCITY

$$v = \frac{Q}{\rho A}$$

3 DARCY FRICTION FACTOR

$$f = \frac{64}{Re}$$

CONSTANTS

$$Q = \text{flow rate} = 0.01 \text{ kg/s}$$

$$\rho = \text{density} = 1000 \text{ kg/m}^3$$

$$\mu = \text{dynamic viscosity} = 1.002 \times 10^{-3} \text{ Pa}\cdot\text{s}$$

$$L = \text{total pipe length} = 6.37984 \text{ m}$$

2 REYNOLDS NUMBER

$$Re = \frac{\rho v d}{\mu}$$

4 DARCY-WEISBACH EQUATION

$$\Delta P_{major} = f \cdot \frac{L}{d} \cdot \frac{\rho v^2}{2}$$

VARIABLES

$$v = \text{flow velocity (m/s)}$$

$$A = \text{pipe's cross-sectional area (} A = \frac{\pi d^2}{4} \text{)}$$

$$d = \text{pipe diameter (m)}$$

$$f = \text{Darcy-Weisbach friction factor}$$

VARIATION 3 (d=0.01)

$$v = \frac{0.01}{1000 \times \frac{\pi(0.01)^2}{4}} = 0.1273 \text{ m/s}$$

$$Re = \frac{1000 \times 0.1273 \times 0.01}{1.002 \times 10^{-3}} = 1270.46$$

$$f = \frac{64}{1270.46} = 0.0504$$

$$\Delta P_{major} = 0.0504 \cdot \frac{6.37984}{0.01} \cdot \frac{1000 \times 0.1273^2}{2} = 260.46 \text{ Pa}$$

$$\frac{R}{d} = \frac{0.0075}{0.01} = 0.75 \quad \text{Using the graph, the corresponding loss coefficient value would be } \sim 0.65.$$

$$\Delta P_{minor} = 0.65 \cdot 14 \cdot \frac{1000 \times 0.1273^2}{2} = 73.76 \text{ Pa}$$

$$\Delta P_{total} = 260.46 + 73.76 = 314.22 \text{ Pa}$$

HEAT TRANSFER OF PLATE

Does not account for air convection or heat spreading, leading to higher temperature predictions. Final values should be taken as a "worst-case scenario" due to its overprediction.

GENERAL METHOD

1 BATTERY HEAT GENERATION

$$Q = q \times V$$

2 TEMPERATURE OF WATER OUTLET

By assuming steady-state conditions and no convection between the plate and the air, all heat is absorbed by the fluid.

$$Q = \dot{m}c_p(T_{outlet} - T_{inlet})$$

$$T_{outlet} = \frac{Q}{\dot{m}c_p} + T_{inlet}$$

VARIATION 1 (d=0.007)

$$Q = 103113 \times 0.42 \times 0.21 \times 0.07 = 636.62W$$

$$T_{outlet} = \frac{636.62}{0.01 \times 4184} + 20 = 35.21^\circ C$$

$$R_{battery} = \frac{0.07}{30 \times 0.42 \times 0.21} = 0.0265K/W$$

$$R_{plate} = \frac{0.01}{154 \times 0.44 \times 0.23} = 0.000642K/W$$

$$Nu = 1.86 \times (1815.28 \times 6.2 \times \frac{0.007}{6.37984})^{\frac{1}{3}} = 4.30$$

$$R_{fluid} = \frac{1}{\frac{4.30 \times 0.6}{0.007} \times \pi \times 0.007 \times 6.37987} = 0.0193K/W$$

$$R_T = 0.0265 + 0.000642 + 0.0193 = 0.046442K/W$$

$$T_{battery-max} = 632.62 \times 0.046442 + 20 = 49.6^\circ C$$

3 CONDUCTION RESISTANCE (BATTERY & PLATE)

$$R = \frac{L}{kA}$$

4 CONVECTION RESISTANCE (FLUID)

$$R = \frac{1}{hA} \quad h = \frac{Nu \cdot k}{d}$$

Since all design variations have a Reynolds number of less than 3000:

$$Nu = 1.86(RePr \frac{d}{L})^{\frac{1}{3}} (\frac{\mu}{\mu_w})^{0.14}$$

5 TOTAL THERMAL RESISTANCE

$$R_T = R_{battery} + R_{plate} + R_{fluid}$$

6 MAXIMUM BATTERY TEMPERATURE

$$T_{battery-max} = QR_T + T_{inlet}$$

CONSTANTS

$$q = 103113 \text{ W/m}^3$$

$$c_p = \text{specific heat capacity} = 4184 \text{ J/kg}\cdot\text{K}$$

$$T_{inlet} = 20^\circ C$$

$$k_{battery} = 30 \text{ W/m}\cdot\text{K}, k_{plate} = 154 \text{ W/m}\cdot\text{K}$$

VARIATION 2 (d=0.008)

$$Q = 103113 \times 0.42 \times 0.21 \times 0.07 = 636.62W$$

$$T_{outlet} = \frac{636.62}{0.01 \times 4184} + 20 = 35.21^\circ C$$

$$R_{battery} = \frac{0.07}{30 \times 0.42 \times 0.21} = 0.0265K/W$$

$$R_{plate} = \frac{0.01}{154 \times 0.44 \times 0.23} = 0.000642K/W$$

$$Nu = 1.86 \times (1588.37 \times 6.2 \times \frac{0.008}{6.37984})^{\frac{1}{3}} = 4.30$$

$$R_{fluid} = \frac{1}{\frac{4.30 \times 0.6}{0.008} \times \pi \times 0.008 \times 6.37987} = 0.0193K/W$$

$$R_T = 0.0265 + 0.000642 + 0.0193 = 0.046442K/W$$

VARIATION 3 (d=0.01)

$$Q = 103113 \times 0.42 \times 0.21 \times 0.07 = 636.62W$$

$$T_{outlet} = \frac{636.62}{0.01 \times 4184} + 20 = 35.21^\circ C$$

$$R_{battery} = \frac{0.07}{30 \times 0.42 \times 0.21} = 0.0265K/W$$

$$R_{plate} = \frac{0.012}{154 \times 0.44 \times 0.23} = 0.000770K/W$$

$$Nu = 1.86 \times (1270.46 \times 6.2 \times \frac{0.01}{6.37984})^{\frac{1}{3}} = 4.30$$

$$R_{fluid} = \frac{1}{\frac{4.30 \times 0.6}{0.01} \times \pi \times 0.01 \times 6.37987} = 0.0193K/W$$

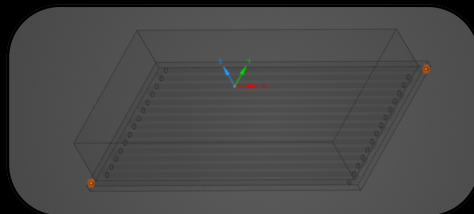
$$R_T = 0.0265 + 0.000770 + 0.0193 = 0.046570K/W$$

$$T_{battery-max} = 632.62 \times 0.046570 + 20 = 49.6^\circ C$$

CFD SETUP

1 EXTRACT VOLUME

The fluid domain is extracted from the pipeline geometry, allowing for fluid parameters to be set.



2 FLUID FLOW CONDITIONS

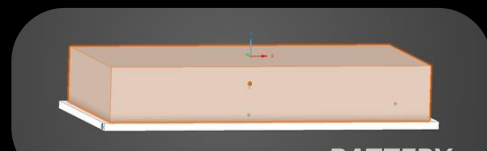
Fluid flow conditions describe the properties of the fluid in the pipeline, particularly at the inlet and outlet:

- Inlet mass flow rate: **0.01 kg/s**
- Outlet pressure: **0 Pa**
- Initial fluid temperature: **25°C**

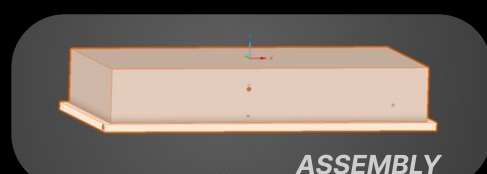


3 SOLID THERMAL CONDITIONS

Solid thermal conditions describe the properties of the fluid in the pipeline, particularly at the inlet and outlet:



BATTERY



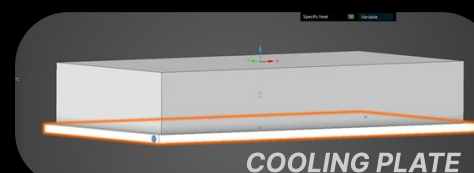
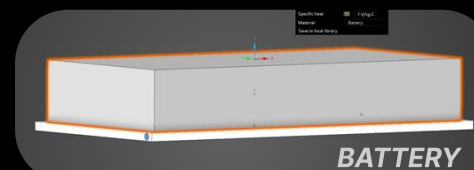
ASSEMBLY

Heat power generation of the battery is set to **103113 W/m³**

Convection occurs in the entire geometry and is set to **5 W/m²•°C** at **25°C**.

4 MATERIAL CONDITIONS

Material conditions describe the physical properties of the battery, cooling plate and fluid:



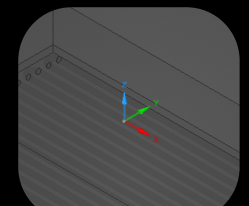
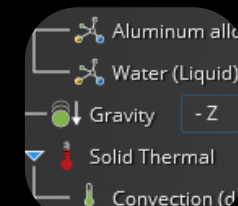
- Density: **2530 kg/m³**
- Thermal conductivity: **30 W/m•K**
- Specific heat: **100 J/kg•K**

Aluminium alloy, wrought, 6061, T4

Fluid is set to water (liquid).

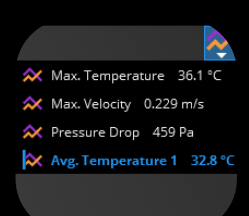
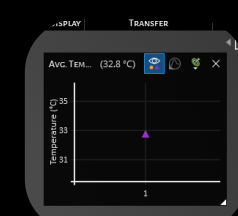
5 GRAVITY

Gravity is set in the -Z direction to simulate real-world conditions.



6 MONITOR

Monitors are set up to track pressure drop, maximum velocity and maximum & average temperature.

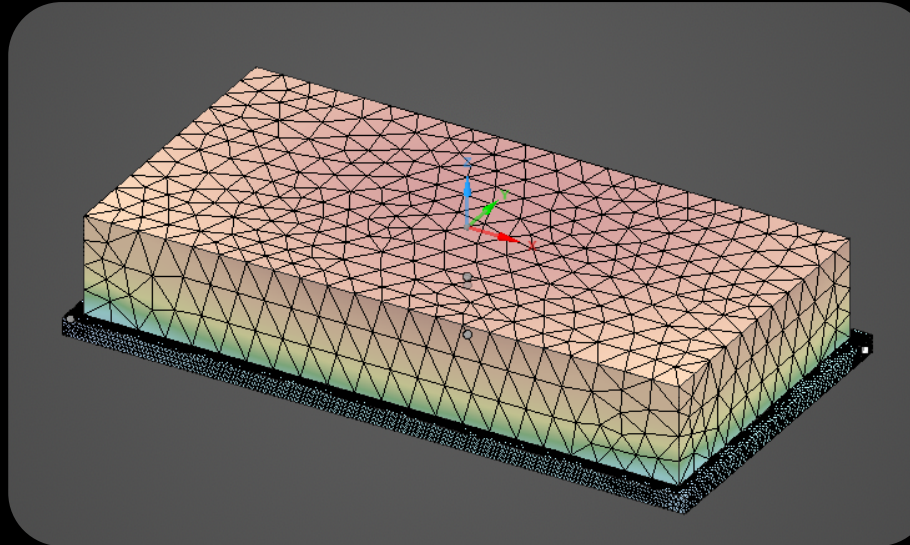


MESHING

Meshing allows for an accurate simulation by **discretising** the vehicle into well-defined cells. Based on the **Turbulent k- ω SST model** used in the CFD simulation, the meshing algorithm automatically refines certain areas accordingly.

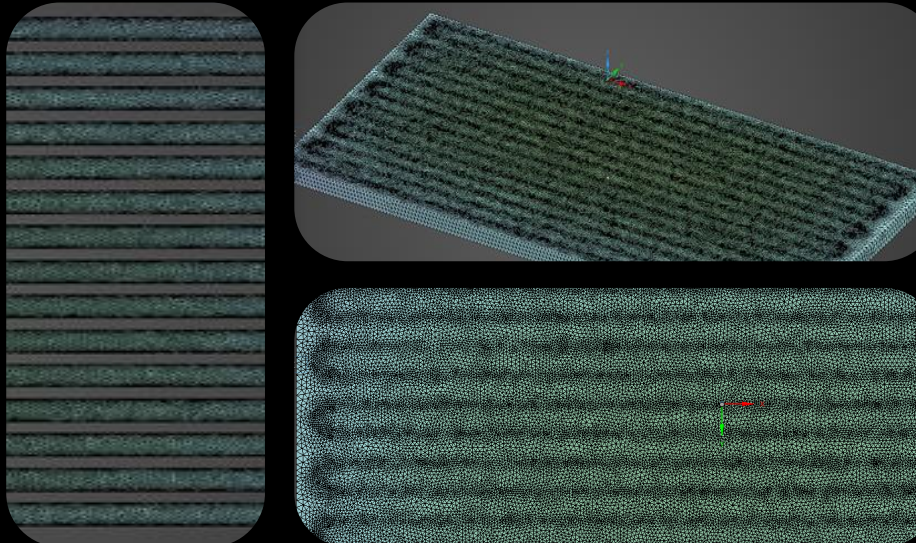
BATTERY MODULE

As conduction is the primary heat transfer in the battery module, it is meshed with an **coarse unstructured tetrahedral mesh**. Contrary to turbulent fluid flow, conduction results in **smoother temperature gradients**. Using a fine mesh would increase the number of elements, therefore increasing the **computational cost** without improving **accuracy** significantly.



COOLING PLATE PIPELINE

In contrast, the a **fine tetrahedral mesh** is used in the pipeline. The **Turbulent k- ω SST model** requires high resolution in boundary layers to accurately capture the **steep temperature gradients, pressure drops and velocity** of the fluid flow. As shown in the images, the pipe walls have **finer elements** compared to the coarser ones in the pipe channels in order to **optimise computational efficiency** without sacrificing key flow information.



MESH COUNT

Design Variation 1



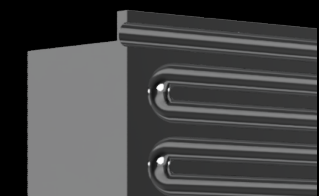
Elements: **4,200,353**
Nodes: **1,151,497**

Design Variation 2



Elements: **3,419,290**
Nodes: **984,854**

Design Variation 3



Elements: **2,721,074**
Nodes: **805,199**

CFD OUTPUTS: PRESSURE LOSS

PRESSURE LOSS COMPARISON

Design Variation	Inlet Pressure (Pa)	Outlet Pressure (Pa)	Pressure Loss (Pa)	Maximum Velocity (m/s)
10mm plate 7mm pipeline	2182	42	2140	0.432
10mm plate 8mm pipeline	1210	30	1180	0.340
12mm plate 10mm pipeline	470	11	459	0.229

PRESSURE PLOT ANALYSIS

The pressure plots on the right obtained from the CFD analysis show **minimal visual difference** between variations. Design Variation 1 was not included as it looked exactly the same as Design Variation 2. However, numerical pressure data is significantly different.

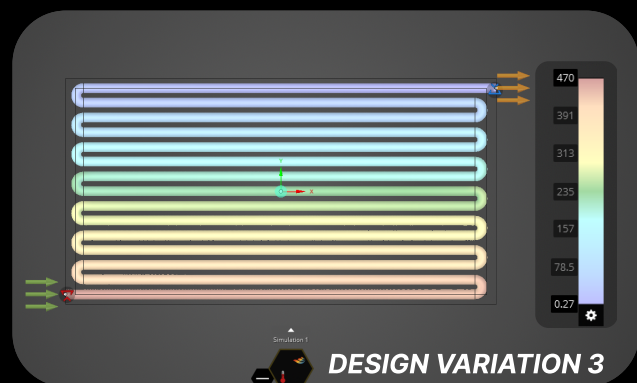
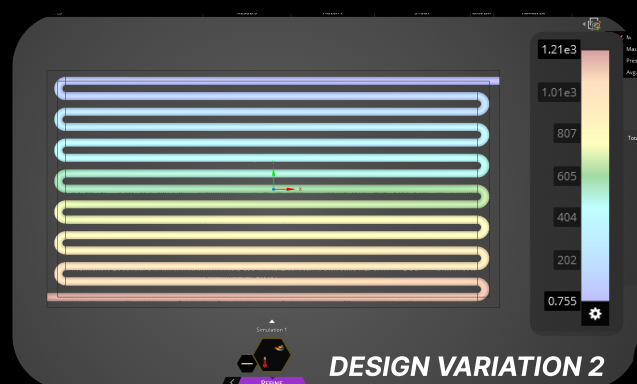
Smaller pipeline diameters result in **higher inlet pressure** and **greater pressure loss**. The smaller cross-sectional area leads to **increased resistance and frictional losses**.

Larger pipeline diameters result in **lower pressure loss**. However, this also leads to a lower flow velocity, possibly reducing cooling efficiency. Further analysis into flow characteristics must be done to determine the trade-off.

KEY FINDINGS

- As the pipeline **diameter increases**, pressure loss and maximum velocity **decreases**.
- This leads to a **trade-off between cooling efficiency and pressure loss**:
 - Lower pressure drop is ideal to **reduce energy consumption**.
 - However a lower velocity can lead to **inefficient heat transfer**.
- Hence, analysing heat transfer results is crucial to deciding which variation is **optimal**.

PRESSURE PLOTS



CFD OUTPUTS: HEAT TRANSFER

HEAT TRANSFER COMPARISON

Design Variation	Maximum Temperature (°C)	Average Temperature (°C)
10mm plate 7mm pipeline	36.4	32.9
10mm plate 8mm pipeline	36.2	32.8
12mm plate 10mm pipeline	36.1	32.8

HEAT TRANSFER PLOT ANALYSIS

The 2D and 3D heat transfer plots on the right were obtained from the CFD analysis of **Design Variation 3** (12mm plate 10mm pipeline). As there was **minimal visual difference** between variations, only the results for the third variation are shown as a representation.

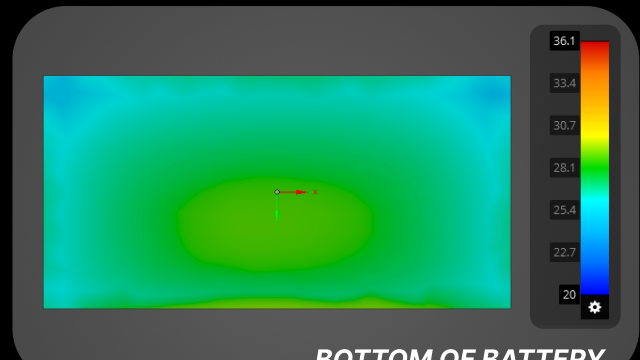
The 2D views of the bottom of the battery and cooling plate show a relatively **uniform temperature distribution**, with slight variations in the centre. This suggests **efficient heat dissipation** which validates my design's cooling abilities.

The 3D view highlights that the top of the battery has the **highest temperature**, which is expected due lack of direct cooling. However, the **temperature gradient** shows evidence of heat dissipation which can be improved further.

KEY FINDINGS

- As the pipeline **diameter increases**, the **maximum temperature decreases** slightly.
- However, the average temperature remains around the same for all three designs, showing that pipeline diameter size has only a **slight impact** on the overall cooling efficiency.
- Overall, the cooling plate design keeps the temperature **below the target value of 40°C**, suggesting that the **Serpentine Pipeline Design** is **efficient** at cooling the battery module.

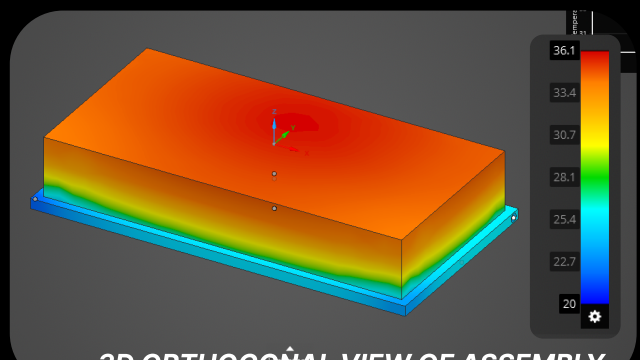
HEAT TRANSFER PLOTS



BOTTOM OF BATTERY



BOTTOM OF COOLING PLATE



3D ORTHOGONAL VIEW OF ASSEMBLY

RESULTS & IMPROVEMENTS

PRESSURE LOSS

CFD results for pressure loss followed the trend predicted from hand calculations. However, they were higher in value, leading to around a **30-40%** disparity between values. Reasons for the discrepancy may include:

- Differences in **Loss Coefficient Values**
- **Turbulence** near inlets and outlets
- **Simplification** of boundary layer effects in hand calculations
- Pipe roughness is **neglected** in hand calculations
- Assumption of **uniform flow** in hand calculations

HEAT TRANSFER

CFD results for heat transfer showed **little variation** between designs, as predicted in hand calculations. As expected, the CFD results showed lower maximum temperatures with a disparity of around **37%**. Reasons for the discrepancy may include:

- Hand calculations use a standard **1D heat transfer model**, whereas in reality, heat transfer is **multidimensional**
- Air convection effects are **neglected** in hand calculations
- Model assumes a **perfectly steady-state condition**
- Contact resistance between the battery and the plate is **neglected**
- Assumption of **uniform flow** in hand calculations

POTENTIAL IMPROVEMENTS

DIFFERENT MATERIAL

- A material with **higher thermal conductivity** could improve the heat dissipation.
- This could improve the temperature gradients within the battery.

MANIFOLDS

- Manifolds at the inlet and outlet could lead to a reduced pressure drop, thus increasing flow uniformity.
- This could lead to more **evenly distributed cooling** throughout the pipeline.

INCREASE PIPE DIAMETER & FLOW RATE

- It is important to keep in mind that there is a **trade-off between pressure loss and cooling efficiency**. Large pipe diameters reduce pressure loss, but may **reduce cooling efficiency** due to lowered velocity.
- Hence, a potential solution may be to increase pipe diameter alongside increasing flow rate, in order to **ensure adequate velocity throughout the pipeline**.

CONCLUSION

CFD OUTPUTS COMPARISON

Design Variation	Pressure Loss (Pa)	Maximum Velocity (m/s)	Maximum Temperature (°C)	Average Temperature (°C)
10mm plate 7mm pipeline	2140	0.432	36.4	32.9
10mm plate 8mm pipeline	1180	0.340	36.2	32.8
12mm plate 10mm pipeline	459	0.229	36.1	32.8

SUMMARY

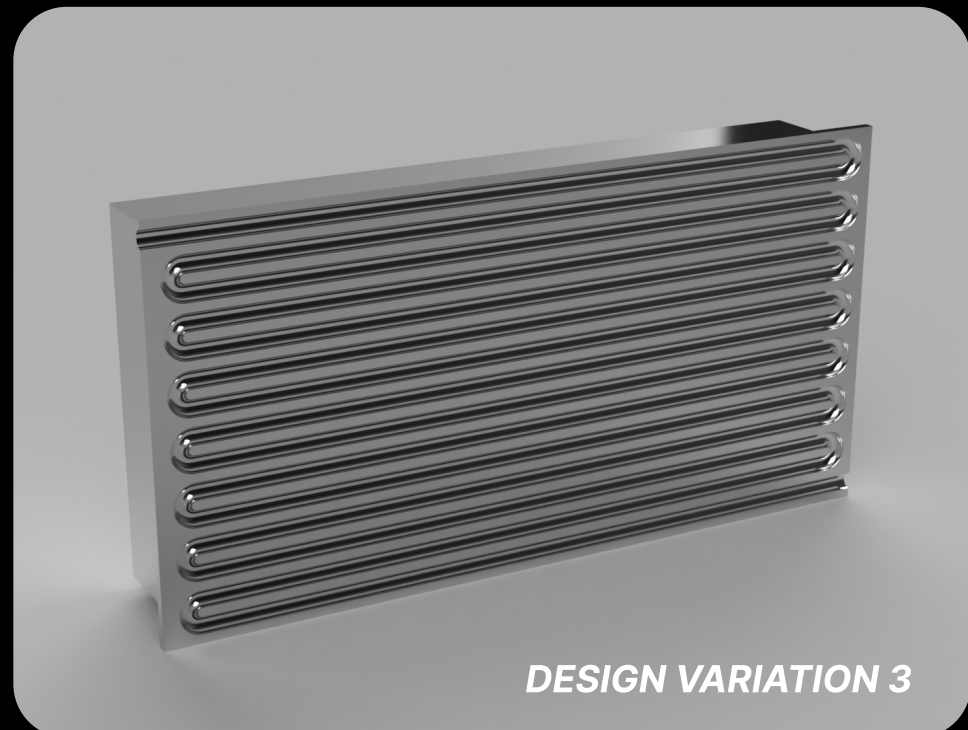
Overall, the Serpentine Pipeline Model with the incorporation of U-bends exhibits **effective cooling efficiency**, achieving the aim to maintain the battery **below 40°C**.

Hand calculations gave valuable insights into pressure loss and heat transfer trends for **design optimisation**. It also provided an estimate of the values that would be obtained from the CFD simulation, with around a **30% disparity**.

DESIGN CHOICE JUSTIFICATION

Design Variation 3 (12mm plate, 10mm pipe diameter) was the most efficient design due to its significantly lower pressure loss while maintaining similar cooling performance.

- Lower pressure loss **reduces energy consumption**
- Lowered velocity **increases system longevity** by reducing turbulence and wear



REFERENCES

- Brunner, C.E., Kiefer, J., Hansen, M.O.L. & Hultmark, M. (2021) Study of Reynolds number effects on the aerodynamics of a moderately thick airfoil using a high-pressure wind tunnel. *Experiments in Fluids*. 62 (8), 178. doi:[10.1007/s00348-021-03267-8](https://doi.org/10.1007/s00348-021-03267-8). [Accessed 24 March 2025].
- Hazeri, K. (2021) Thermofluids: Energy & Design. Introduction to Heat Transfer [Notes] Imperial College London [Accessed: 20 March 2025]
- Hazeri, K. (2022) Thermofluids: Energy & Design. Pipe Flow [Notes] Imperial College London [Accessed: 20 March 2025]
- He, R., Sun, H., Gao, X. & Yang, H. (2022) Wind tunnel tests for wind turbines: A state-of-the-art review. *Renewable and Sustainable Energy Reviews*. 166 (C). <https://ideas.repec.org/a/eee/reneus/v166y2022ics1364032122005664.html>. [Accessed: 12 March 2025].
- Imperial College London (n.d.d) T1 and T2 Wind Tunnels | Faculty of Engineering. <https://www.imperial.ac.uk/aeronautics/research/facilities/t1-andt2/> [Accessed: 12 March 2025].
- Jayanti, S. (2011) Bends, Flow and Pressure Drop in. In: Thermopedia. Begel House Inc. p. doi:[10.1615/AtoZ.b.bends_flow_and_pressure_drop_in](https://doi.org/10.1615/AtoZ.b.bends_flow_and_pressure_drop_in). [Accessed 21 March 2025].
- Nasa (n.d.e) The Lift Coefficient. <https://www.grc.nasa.gov/www/k-12/VirtualAero/BottleRocket/airplane/liftco.html> [Accessed: 18 March 2025].
- The Engineering ToolBox (2004). Darcy-Weisbach Equation: Flow Resistance & Pressure Loss Calculator. [online] Available at: https://www.engineeringtoolbox.com/darcy-weisbach-equation-d_646.html [Accessed 21 March 2025].
- ScienceDirect (n.d.c) Laminar Boundary Layer - an overview <https://www.sciencedirect.com/topics/physics-and-astronomy/laminar-boundary-layer> [Accessed: 21 March 2025].
- SimScale (n.d.b) K-Omega Turbulence Models | Global Settings. <https://www.simscale.com/docs/simulation-setup/global-settings/k-omega-sst/> [Accessed: 21 March 2025].